Deterministic chaos and dynamical instabilities in a multimode cw dye laser

H. Atmanspacher and H. Scheingraber
Institut für Extraterrestrische Physik, Max-Planck-Institut für Physik und Astrophysik, D-8046 Garching bei München, Federal Republic of Germany
(Received 13 January 1986)

The dynamics of a cw pumped, multimode dye laser system have been experimentally investigated by measuring the mode correlation times t_{mode}, the second-order dimension D_2 of the attractor of the system, and the corresponding second-order entropy K_2. Dynamical instabilities have been observed as discontinuous changes of t_{mode}, D_2, and K_2 at distinct values of the spectral power density $P/\Delta\lambda$. Over the whole investigated range of $P/\Delta\lambda$, the analysis of the experimental data yields sufficient conditions for deterministic chaos. The dimensionality of the system and its degree of chaos have been found to depend on the spectral power density. The contributions of stochastic and of chaotic processes to the limited mode correlation time have been unraveled.

I. INTRODUCTION

Deterministic chaos and instabilities in synergetic systems have increasingly become subjects of advanced interest.[1] A fundamental reason for this interest arises from the fact that both phenomena severely affect our understanding of dynamic processes in nature. The concepts of complete determinism and strong causality are reduced to the "special-case level" of systems in thermal equilibrium. These concepts are therefore irrelevant for describing *any* evolutionary processes which require situations far from thermal equilibrium.

Quantum optical systems like lasers are rather suitable examples in order to study processes which develop far from thermal equilibrium. Compared with chemical or even biochemical systems, the complexity of laser systems is still on an elementary level. However, they are complicated enough that no complete theoretical treatment of the wide variety of observations is available until now. Review articles of Abraham *et al.*[2] (instabilities in laser systems) and of Ackerhalt *et al.*[3] (chaos in quantum optics) stress this situation.

From an experimental point of view, there are two possibilities to get clear evidence for chaotic behavior. The first one is to observe one of the commonly known transition scenarios to chaos (i.e., period doubling, intermittency, or the Ruelle-Takens scenario). For various types of lasers, observations of these scenarios have already been reported.

The second possibility to gain information whether a dynamical system behaves chaotically is to determine invariants of the system which directly characterize chaotic behavior. Two invariants of this kind are easily extractable from experimental data.

(1) The dimension of the attractor of the system in phase space.

(2) The entropy which is connected with the evolution of the system in phase space.

Of course, these invariants are meant to be temporal invariants under constant boundary conditions. They may change, if some control parameter of the system is varied. In case of laser systems, the pump power serves as an appropriate control parameter. At certain critical values of the pump power, the attractor of the system can become unstable. The system then switches into another attractor with different dimension and entropy. Such a transition is called a dynamical instability. It can be understood analogous to a thermodynamical phase transition, whose occurrence is limited to situations in thermal equilibrium.

The most important dynamical instability which appears in laser systems is the lasing threshold, where stimulated emission starts to dominate over spontaneous emission. By means of this change, coherent radiation in one of more different cavity modes is established. However, even within the regime of coherent radiation higher-order instabilities may occur. General correspondence criteria for such instabilities in single-mode and multimode lasers have recently been evaluated by Lugiato and Narducci.[4]

Higher instabilities have been observed in a homogeneously broadened ring dye laser by Hillman *et al.*[5] Not far above the laser threshold, a discontinuous increase of the average output power occurred, connected with a simultaneous alteration of the mode structure from single-mode operation to two-mode operation of symmetric sidebands. A first attempt of a theoretical description of these phenomena has been carried out by Lugiato *et al.*[6]

In another experiment by Westling *et al.*[7] a linear multimode dye laser also showed an instability not far above the laser threshold. This instability was discovered by measuring the autocorrelation of the total laser output, which showed a discrete jump at a certain pump power.

In a recent paper (hereafter referred to as paper I),[8] we proposed a novel method to determine the correlation times of individual longitudinal modes in a cw pumped multimode laser by means of intracavity absorption. It turned out that the mode correlation times in the investigated linear multimode laser generally decrease with increasing spectral power density inside the laser cavity. However, a detailed observation revealed discontinuities in the mode correlation times at certain critical spectral power densities. This kind of instability obviously differs from the instabilities mentioned above, since the discon-

tinuities appear as a function of the spectral power density, and not as a function of the pump power. We shall particularly discuss this difference in Sec. IV B.

The investigations described in paper I left the question open of whether deterministic chaos contributes to the behavior of the laser system. It is the purpose of the present paper to give clear experimental evidence that deterministic chaos plays a significant role in the dynamical behavior of cw pumped multimode laser systems. The degree of chaos can be classified by the invariants mentioned above. The underlying theoretical concepts are reviewed in Secs. II A and II B. The extraction of the invariants from experimental data will be explained in Sec. II C. The experimental details are described in Sec. III. In Sec. IV we discuss the dependence of the mode correlation times, the attractor dimension, and the corresponding entropy on the intracavity spectral power density. An interpretation will be given which describes the mechanism governing the observed instabilities. Analogies with thermodynamical phase transitions will be considered. Moreover, it will be shown how one can distinguish between chaotic and stochastic contributions to the correlation time of individual modes. The results are summarized in Sec. V.

II. DIMENSIONS AND ENTROPIES OF DYNAMICAL SYSTEMS

A. Attractor dimension

The attractor of a dynamical system in phase space can be suitably characterized by two invariants which we introduce according to Procaccia.[9] He treated the dimension of the attractor as well as the corresponding entropy starting from the definition of the qth-order information H_q:

$$H_q=\frac{1}{1-q}\log\sum_i p_i^q \ . \tag{1}$$

The *discrete* probability p_i is defined by $p_i=N_i/N$, where N is the total number of elements in the considered sample space. Given some partition Φ consisting of the elements $\{\Phi_1,\ldots,\Phi_m\}$ in the sample space, one can count how many times N_i an element is found in Φ_i. According to fundamental information theory, we use the logarithm to base 2 throughout this paper.

Now we take the basin of an attractor as a sample space and consider a finite partition $\Phi(r)$ with diameter r of this basin, in which the trajectory $\mathbf{X}(t)$ is situated. Then

$$H_q(r)=\inf_{\Phi(r)}H_q(\Phi(r)) \tag{2}$$

denotes a qth-order information which depends on the partition diameter r. $H_q(r)$ is given by the infimum of the different informations resulting from all possible partitions $\Phi(r)$.

With Eq. (2), one can define a quantity D_q of order q,

$$D_q=-\lim_{r\to 0}\frac{H_q(r)}{\log r} \ , \tag{3}$$

which is the (generalized) qth-order dimension of the attractor.

With respect to experimental applications, the most useful dimensions are of low order. $D_0=\lim_{q\to 0}D_q$ is the *fractal dimension* of the attractor:

$$D_0=-\lim_{r\to 0}\frac{\log M(r)}{\log r} \ . \tag{4}$$

It is determined by $M(r)$, the minimal number of cubes with edge length r needed to cover the attractor. Equation (4) is equivalent to Mandelbrot's definition of the fractal dimension,[10] which originates from Hausdorff.[11]

The first-order dimension $D_1=\lim_{q\to 1}D_q$ is the *information dimension*, since it is based on the commonly known first-order information $S(r)$:

$$D_1=\lim_{r\to 0}\frac{S(r)}{\log r} \tag{5}$$

with

$$S(r)=-\sum_{i=1}^{M(r)} p_i\log p_i \ . \tag{6}$$

The second-order dimension

$$D_2=\lim_{r\to 0}\frac{\log C(r)}{\log r} \tag{7}$$

has been introduced as the *correlation exponent* by Grassberger and Procaccia.[12] It is obtained by the function

$$C(r)=\lim_{N\to\infty}\frac{1}{N^2}\sum_{i,j=1}^{N}\Theta(r-|\mathbf{X}_i-\mathbf{X}_j|) \ . \tag{8}$$

Θ is the Heaviside function: $\Theta(x)=0$ for $x\le 0$ and $\Theta(x)=1$ for $x>0$. The function $C(r)$ counts the number of pairs of those points with a distance $|\mathbf{X}_i-\mathbf{X}_j|$ smaller than r. The determination of $C(r)$ (and D_2) from experimental data will be described in Sec. II C. Remarkably, $C(r)$ is simply the correlation integral

$$C(r)=\int_0^r d^d r' c(\mathbf{r}') \ , \tag{9}$$

where $c(\mathbf{r})$ is the standard (two-point) correlation function (d is the dimension of the vector space of $\mathbf{r}$). Higher-order correlation functions lead to higher-order dimensions D_q.

It has been shown[12] that $D_2\le D_1\le D_0$. The conditions for the equality of the dimensions are satisfied, if the points are distributed uniformly over the attractor. For several different maps and equation systems, the correlation exponent D_2 has been proven to be nearly identical with D_1 and D_0. In particular, this is true for the Lorenz system,[12] which is formally equivalent with the quantum optical Maxwell-Bloch equations.[13] Therefore, D_2 is a very useful tool for estimating the information dimension and the fractal dimension of an attractor.

B. Trajectory entropy

The qth-order dimensions of an attractor are *static* invariants, since they do not depend on any time scale. However, the entropy of a system is always a quantity which has to be specified per time unit (if it is not zero or infinite). Therefore it is a *dynamic* invariant describing

properties of a considered *process*. On the contrary, the classical Boltzmann entropy characterizes a *state* in thermal equilibrium.

Procaccia[9] has shown how to define the qth-order entropies by means of the qth-order informations given by Eq. (2). We shall not follow this definition in detail, but give a result similar to Eq. (3) for the qth-order entropy of a trajectory $\mathbf{X}(t)$ situated in the basin of an attractor. The considered points $\mathbf{X}(t)$ along the trajectory are separated by a constant time increment τ. (In an experiment, τ characterizes the temporal resolution of measurement.) The whole phase space is considered to be partitioned into cubes of edge length r. Now, $p(i_1,i_2,\ldots,i_d)$ is the *joint* probability that $\mathbf{X}(t=\tau)$ is in cube i_1, $\mathbf{X}(t=2\tau)$ is in cube $i_2,\ldots,$ and $\mathbf{X}(t=d\tau)$ is in cube i_d. The qth-order entropy is then defined as

$$K_q=-\lim_{r\to 0}\lim_{d\to\infty}\frac{1}{d\tau(q-1)}\log\sum_{i_1,\ldots,i_d}p^q(i_1,\ldots,i_d)\ . \tag{10}$$

This definition includes the fact that K_q has the dimension of $\sec^{-1}$. K_0 is the *topological entropy*.

The first-order entropy $K_1=\lim_{q\to 1}K_q$ is the *metric* or *Kolmogorov entropy* which is a measure for the internal information production of the system during its temporal evolution:

$$K_1=\lim_{r\to 0}\lim_{d\to\infty}\frac{1}{d\tau}\sum_{i_1,\ldots,i_d}p(i_1,\ldots,i_d)\log p(i_1,\ldots,i_d)\ . \tag{11}$$

K_1 is approximately identical with the sum of positive *Lyapunov exponents* of the system.

Similar to the second-order dimension D_2, a second-order entropy K_2 can be defined by the correlation integral $C(r)$ [Eq. (8)]:[14]

$$K_2=\lim_{r\to 0}\lim_{d\to\infty}\frac{1}{\tau}\log\frac{C_d(r)}{C_{d+1}(r)}\ . \tag{12}$$

Its determination from experimental data will be described in Sec. II C. In general, $K_2\le K_1\le K_0$ is valid. The limiting cases $K_1=0$ and $K_1\to\infty$ characterize the situations of *regular* (e.g., periodic) and *stochastic* behavior of the system, respectively. If $K_1>0$, the system shows *chaotic* behavior. Since $K_2\le K_1$, $K_2>0$ is a sufficient condition for deterministic chaos. Furthermore, K_2 can be used to quantify the degree of chaos.

The Kolmogorov entropy K_1 is related to the inverse predictability time (correlation time τ_{corr}) of the behavior of the system.[15] If additional stochastic forces are imposed on the system, the total correlation time of its variables can be shorter than τ_{corr} which is purely due to chaotic behavior.

C. Estimation of dimensions and entropies from a time series

As already indicated in Secs. II A and II B, the correlation exponent D_2 of an attractor and the corresponding second-order entropy K_2 can be estimated from a measured time series of a *single* variable of the system. It is not necessary to measure all n variables $\mathbf{X}_i(t)$ $(i=0,\ldots,n-1)$ of the system. Moreover, even the knowledge of the number n of degrees of freedom (NDF) of the system (i.e., the dimension of the real phase space) is not required. The measurement of a single variable $\mathbf{X}_0(t)$ is sufficient, because it contains all information on the other $(n-1)$ variables by means of the derivatives $d\mathbf{X}_0(t)/dt$.[16]

Of course, an analytical procedure of this kind would not be very practicable. However, the underlying idea can be easily realized, if one constructs d additional data sets from the original time series $\mathbf{X}_0(t)$ instead of its temporal derivatives. The d additional data sets are obtained by introducing a time delay $(k\Delta t)$ for the kth constructed data set. The resulting data sets $\mathbf{X}_0(t),\ldots,\mathbf{X}_0(t+d\Delta t)$ define a d-dimensional phase space, if they represent linearly independent variables.[17]

We stress the fact that the dimension d of the constructed phase space is not identical with the dimension n of the real phase space of the system. In general, one has to choose $d>n$, since the constructed d linearly independent data sets do not describe the system as low dimensional as the real variables: they do not give an irreducible representation. (This is valid for any artificial "basis set" for physical systems.) In order to construct linearly independent data sets, the time delay unit Δt may not be identical with an inverse eigenfrequency of the system.

If each data set contains N values spaced by a time increment τ, the described method reveals the following set of data sets:

$$\begin{aligned}&X_0(t_1) && \ldots X_0(t_N),\\ &X_0(t_1+\Delta t) && \ldots X_0(t_N+\Delta t),\\ &\quad\vdots && \quad\vdots\\ &X_0(t_1+d\Delta t) && \cdots X_0(t_N+d\Delta t).\end{aligned}$$

Within the vector representation

$$\tilde{X}_i=(X_0(t_i),\ldots,X_0(t_i+d\Delta t)) \tag{13}$$

the above given total set becomes

$$\tilde{X}_1,\ldots,\tilde{X}_N\ . \tag{14}$$

Now, for each j one takes the point $\tilde{X}_j$ from (14) and measures the distances $|\tilde{X}_i-\tilde{X}_j|$ between all the other points $\tilde{X}_i$ and $\tilde{X}_j$. (Any convenient distance norm is appropriate, we choose the Euclidean norm.)

In this manner one can determine the number of those pairs of points whose distance is smaller than a given distance r. With this result we can now directly go into the correlation integral $C(r)$ given by Eq. (8). $C(r)$ is the basic quantity needed for the further determination of D_2 according to Eq. (7).

The correlation integral $C(r)$ has to be calculated for several values of r with respect to each particular dimension d of the constructed phase space. For each dimension d one plots $\log C(r)$ versus $\log r$ and obtains a slope ν of the linear range of the resulting curve [because of the $\lim_{r\to 0}$ in Eq. (7) this linear range extends towards small r]. Figure 1 illustrates the mentioned curves for an ex-

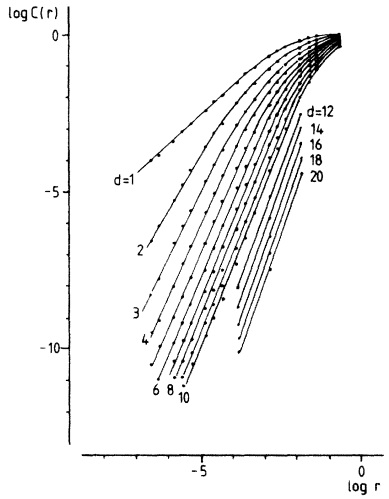

FIG. 1. Log-log plot of the correlation integral $C(r)$ vs the distance r, providing a linear range of the slope according to Eq. (7). With an increasing dimension d of the constructed phase space, the slope converges towards a limiting value. The analysis was based on the temporal evolution of the mode intensity in a multimode laser, recorded at a spectral power density of 515 mW/nm. Other parameter values are $\Delta t=\tau=39$ μsec and $N=512$ points.

perimental situation described in the figure caption.

If the slope ν converges towards a finite value for high d, this value is identical with D_2. In Fig. 2 we illustrate the converging slopes for the curves of Fig. 1, for which one obtains $D_2=2.66$. The errors result from a linear least-squares fit of the calculated values in the linear range. The drawn line with $\nu=d$ represents an example for divergent behavior of $\nu(d)$ which characterizes purely *stochastic* behavior. In the general case of stochastic processes, ν does not reach any limiting value for $d\to\infty$. If D_2 turns out to be an integer, the behavior of the system is *regular* within the considered time scale. Any fractal (noninteger) D_2 is a sufficient criterion for contributions of deterministic chaos to the behavior of the system as long as $D_2\simeq D_0$.

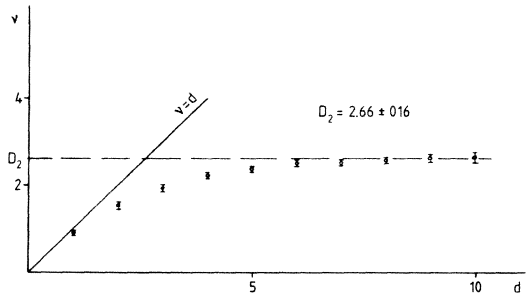

FIG. 2. Slope ν in the linear range of the different curves in Fig. 1, shown as a function of the dimension d of the constructed phase space. The solid line denoted by $\nu=d$ illustrates a completely stochastic behavior where $D_2\to d$. For the analyzed time series (compare Fig. 1), ν reaches a limiting value already in a ten-dimensional phase space. This limiting value is identical with the second-order dimension $D_2=2.66\pm0.16$.

If there would be more than one linear scaling region in each of the curves shown by Fig. 1, it would in principle be possible to distinguish between different kinds of processes occurring in different amplitude ranges of the measured signal. With respect to the discussed procedure, those different amplitude ranges correspond to different ranges of r. For the case of a time series with underlying (stochastic) noise, this has already been demonstrated.[18]

From the obtained value of D_2 it is possible to extract another very valuable piece of information. As mentioned above, the dimension d of the constructed phase space is usually larger than the real NDF of the system. A determined value $D_2=2.66$ by means of the convergence of ν until $d=10$, for example, allows the conclusion that the investigated process needs only the next higher integer NDF (i.e., three) to be successfully modeled.

Every determination of the dimension of an attractor by the described procedure provides some statistical error. This error might possibly prevent a discrimination between an integer or a fractal value of D_q. In this case, the second-order entropy turns out to be very useful, since it provides an additional sufficient condition for chaotic behavior, namely $K_2>0$ (compare Sec. II B).

In order to determine K_2 by means of Eq. (12), the time increment τ between successive data points within each data set has to be taken into account besides the correlation integral $C(r)$. (Note the difference between Δt and τ.) According to Eq. (12), K_2 can be estimated from the vertical distances (at identical r) between the curves belonging to successive dimensions d. [Now d has got a concrete meaning compared with the formal introduction of K_q by Eq. (10).] In Fig. 3 we show how K_2 turns out as a limiting value for high dimension d. The indicated values for each particular d have been calculated from the mean value of $C_d(r)/C_{d+1}(r)$ over the linear range of r. Figure 3 refers to the same experimental situation as Figs. 1 and 2.

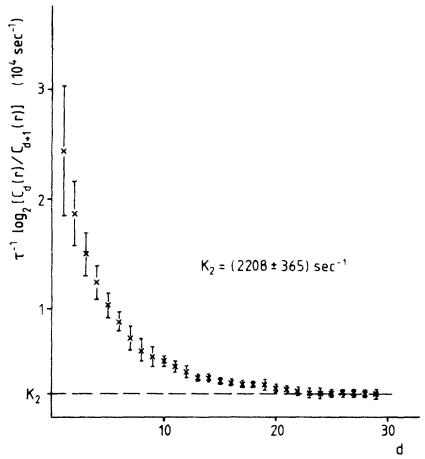

FIG. 3. Mean values of $\tau^{-1}\log_2[C_d(r)/C_{d+1}(r)]$ as a function of d, obtained from the linear range of the curves in Fig. 1. According to Eq. (12), the limiting value for large d gives the second order entropy $K_2=2208\pm365$ sec^{-1}. Compared with the determination of D_2, a considerably higher value of d is needed to reach a convincing convergence.

TABLE I. Dimensions and entropies as sufficient criteria for stochastic, chaotic, and regular behavior of a system. D_0 is the fractal dimension [Eq. (4)], D_2 is the correlation exponent [Eq. (7)], K_1 is the Kolmogorov entropy [Eqs. (11) and (16)], K_2 is the second-order entropy [Eq. (12)], and d is the Euclidean dimension of the constructed phase space according to (14).

	Dimension	Entropy
Regular	$D_2=D_0$ integer	$K_2=K_1=0$
Chaotic	$D_2\simeq D_0$ fractal	$K_2>0$
Stochastic	$D_2\rightarrow d$	$K_2\rightarrow\infty$

For a convenient overview, Table I summarizes the sufficient criteria for stochastic, chaotic, and regular behavior which are given by means of attractor dimensions and entropies.

III. EXPERIMENTAL

Within the context of paper I, we have investigated how the correlation times of longitudinal laser modes depend on the spectral power density $P/\Delta\lambda$ inside the laser cavity. At certain critical values of $P/\Delta\lambda$, discontinuous jumps of the mode correlation times have been observed. In order to gain further information about this kind of dynamical instabilities, we apply the concepts of attractor dimension and entropy.

As indicated in Sec. II C, the experimental determination of the dimension and the entropy of a dynamical system is already possible by an analysis of a single-variable time series. This time series can be used as the data set $X_0(t)$, from which the total set according to (14) has to be constructed. In case of a multimode laser system, the mode intensity is a time-dependent variable which is rather easily accessible from experiment. On the other hand, it is directly related to the mode amplitude which is described by one of the Maxwell-Bloch equations. Hence, the mode intensity is a convenient candidate for the measurement of the required data set.

In addition to the single-variable time series, the correlation times of the longitudinal laser modes have been measured as a function of the spectral power density. For the description of the concerning experimental arrangement and of the applied intracavity absorption method, we refer to paper I. In the following, we treat those details of the experiment, which are important for the measurement of the temporal evolution of the mode intensity.

The 2-m-grating spectrometer used in order to disperse the laser emission spectrum, provides a theoretical resolution of 84 000 in first order, corresponding to a resolution limit of 0.007 nm at a wavelength of 590 nm. Since the actual resolution is usually smaller than the theoretical resolution, we assume a value of 0.01 nm at an optimized entrance slit width of 15 μm. Due to a mode spacing of 250 MHz ($=0.000\,29$ nm), we always observe a superposition of at least 35 longitudinal modes within the spectral resolution of the spectrometer. Increasing the exit slit width of the spectrometer, one can enhance the number of modes which contribute to the measured multiplier signal.

The mode correlation times have been determined from the depths of particular H_2O absorption lines in the laser emission spectrum. These lines were recorded by means of a scanning multiplier in the focal plane of the spectrometer. On the other hand, the temporal evolution of the mode intensities was measured at a fixed multiplier position. For each particular spectral power density, we observed the mode intensity (i) in the center of an absorption line, and (ii) around the maximum of the broadband laser emission.

The measured signal was recorded and digitized by means of a transient digitizer with a time resolution of 512 channels. The signal was normalized with respect to the maximum intensity within the considered time interval. A total time window of 20 msec (corresponding to a temporal resolution of $\tau=39$ μsec) turned out to be a proper value for the data analysis.

Figures 4 and 5 show two examples of a time series over 20 msec, as obtained in the laser-emission maximum at spectral power densities of 118 mW/nm and 208 mW/nm, respectively. With the corresponding data sets the second-order dimension D_2 and entropy K_2 can be determined as described in Sec. II C.

During an extended preanalysis, possible influences of different experimental and numerical boundary conditions on the obtained values of D_2 and K_2 have been investigated.

(1) Reproducibility of D_2 (K_2) from different time series at identical spectral power density. For successive recorded time series at a constant spectral position and with a constant multiplier slit width, we obtained deviations of D_2 and K_2 which reached about three times the statistical error of a particular measurement. Therefore, it was necessary to consider more than one individual time series for obtaining a reasonable mean value of D_2 (K_2). In order to avoid confusion, we point out that the determination of D_2 (K_2) in Figs. 2 and 3 is based only on one single time series. In contrast to this, the values discussed in Sec. IV represent mean values in the sense explained above.

(2) Dependence of D_2 (K_2) on the number of simul-

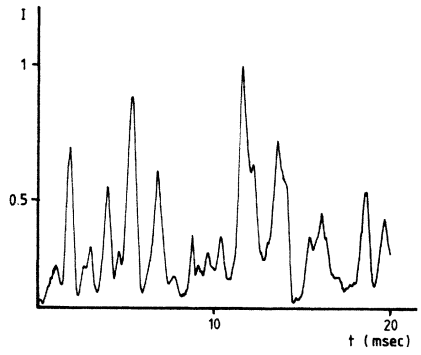

FIG. 4. Temporal evolution of the normalized mode intensity I, recorded at the maximum intensity of the broadband laser emission. Over the total time interval of 20 msec, one notices a clearly irregular behavior. The shown time series has been obtained at a spectral power density of 118 mW/nm with a time resolution of $\tau=39$ μsec. The extracted values of $D_{2,\max}$ and $K_{2,\max}$ are given in Figs. 6 and 7.

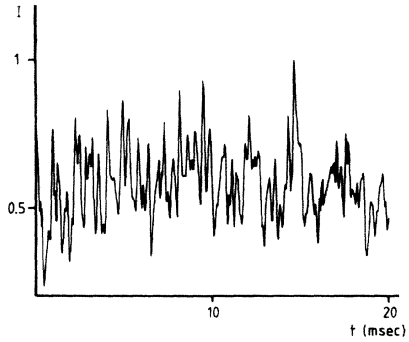

FIG. 5. Same as in Fig. 4, for a spectral power density of 208 mW/nm. The temporal behavior of the normalized mode intensity I is clearly more irregular than in Fig. 4. The calculated values of $D_{2,\max}$ and $K_{2,\max}$ can be seen in Figs. 6 and 7.

taneously observed modes. As already mentioned, due to the limited resolution of the spectrometer the observed signal represents an average over at least 35 longitudinal laser modes. Of course, this is a very small number compared with a total number of some thousand modes which correspond to typical emission bandwidths. Nevertheless, we tried to find discrepancies in the determination of D_2 and K_2 due to different numbers of simultaneously recorded modes. Different numbers of modes could be realized by different multiplier slit widths at the same optimized entrance slit width of the spectrometer. Compared with the error resulting from point (1), no significant change of D_2 (K_2) could be detected. For this reason, we assumed the maximum resolution (35 modes) to provide an appropriate "single-variable" time series of the laser system. If a better resolution would have been necessary, we would expect significantly different correlations $C(r)$ [compare Eq. (8)] in phase space for different numbers of modes. This would lead to different values of D_2 (K_2).

(3) Dependence of D_2 (K_2) on the temporal resolution τ of the measured time series. Generally, τ should be taken such that a sequence of some data points falls within the characteristic time scale of the system under investigation. If τ is considerably larger than this time scale, successive data points can naturally not show any correlation. Hence, the analysis of the time series will clearly reveal the criteria for uncorrelated (stochastic) behavior. On the other hand, if τ is very small, the influence of counting statistics on the results of the analysis increases. In this case, a stochastic behavior may be pretended due to the statistics of the measuring procedure. In our experimental situation, the choice of an appropriate τ is unproblematic since the characteristic time scale of the system is experimentally available by the mode correlation time. This time scale is about some 100 μsec. The analysis of several particular data sets with temporal resolutions $\tau=9.75$, 19.5, and 39 μsec revealed identical values for D_2 (K_2). Since τ appears explicitly in Eq. (12) which defines K_2, a constant value of K_2 at different τ supports the self-consistency of the applied method. For the final analysis, $\tau=39$ μsec has been used. This temporal resolution corresponds to a total time window of 20 msec for each recorded time series.

(4) Dependence of D_2 (K_2) on different time delays Δt. As described in Sec. II C, the original, experimentally obtained data set $\mathbf{X}_0(t)$ is used to construct d linearly independent data sets by means of a time delay Δt. If Δt would unfortunately equal an inverse eigenfrequency of the system, the constructed total data set would consist of linearly dependent variables. Therefore, it would always give rise to a one-dimensional phase space in which an increase of d (the number of linearly dependent variables) could never lead to a correlation exponent $D_2 > 1$. Hence, a correlation exponent $D_2 > 1$ is sufficient to exclude the case of a total data set which consists of linearly dependent variables. We performed the analysis of several particular data sets for $\Delta t = \tau$, 2τ, and 3τ. In all three cases the obtained correlation exponent $D_2 > 2$ did not remarkably change for different Δt. For the final analysis we took $\Delta t = \tau$ in order to keep as many data points as possible for the constructed total data set. For example, $\Delta t = 10\tau$ would reduce the original 512 data points to $512 - 10d$ data points due to Eqs. (13) and (14). Such a reduced data set can offer severe problems in obtaining a useful linear range of $\log C(r)$ versus $\log r$. With a number of about 500 points which results from $\Delta t = \tau$, we could carry out the analysis without problems.

(5) Dependence of D_2 (K_2) with respect to emission maxima and absorption dips. At high spectral power densities, no significant discrepancies have been observed. However, in the case of low spectral power densities, the value of $D_{2,\text{abs}}$ as measured in the center of an absorption line always exceeded the value of $D_{2,\max}$ as measured in the laser-emission maximum. Similarly, $K_{2,\text{abs}}$ was significantly larger than $K_{2,\max}$. Hence, at low spectral power densities it was necessary to take different time series for the emission maximum and for absorption dips, respectively. In Sec. IV, we shall return to this remarkable difference.

IV. RESULTS AND DISCUSSION

A. Dimensions and entropies as a function of $P/\Delta\lambda$

As already indicated in paper I, the investigation of chaotic properties of multimode laser systems promises an advanced understanding of the dynamical instabilities reported in paper I. This kind of instability has been observed by means of a discontinuous decrease of the mode correlation times at certain critical spectral power densities. Therefore, we determined the attractor dimension D_2 and the trajectory entropy K_2 over a range of $P/\Delta\lambda$ in which those instabilities occurred. This range was selected by means of a quick survey of the mode correlation times as a function of $P/\Delta\lambda$. It turned out that two discontinuities of the mode correlation times appeared between 110 and 210 mW/nm at the particular cavity adjustment. In order to investigate the behavior of D_2 and K_2 in the mentioned range of $P/\Delta\lambda$, four time series have been recorded and analyzed for each particular spectral power density. Since the range between 110 and 210 mW/nm contains low spectral power densities, it was necessary to distinguish between $D_{2,\max}$ ($K_{2,\max}$) and

$D_{2,\mathrm{abs}}$ ($K_{2,\mathrm{abs}}$) as pointed out in Sec. III. The total number of four time series contained (i) two time series recorded at the spectral position of an absorption line, and (ii) two time series recorded at the spectral position of the laser emission maximum.

In Fig. 6, we show the mean values of the correlation exponent $D_{2,\mathrm{max}}$ in the mentioned region of low spectral power densities together with the corresponding errors [see point (1) of Sec. III]. On the horizontal axis, the critical values $(P/\Delta\lambda)_{\mathrm{crit}}$ are indicated as obtained by the quick survey of the mode correlation times. The two values of $(P/\Delta\lambda)_{\mathrm{crit}}$ are 135 and 185 mW/nm, both with an uncertainty of ± 0.5 mW/nm. These critical power densities separate three ranges of $P/\Delta\lambda$. For each one of these ranges a mean value for $D_{2,\mathrm{max}}$ is indicated (drawn as a dashed line) which results from the particular values of $D_{2,\mathrm{max}}$ in the considered range of $P/\Delta\lambda$. Table II gives the mean values of $D_{2,\mathrm{max}}$ in the different ranges together with their statistical errors.

The noninteger, fractal values of $D_{2,\mathrm{max}}$ are a first indication of chaotic behavior of the multimode system in the investigated range of $P/\Delta\lambda$. According to the sufficient conditions for chaos summarized in Table I, we stress the fact that a fractal D_2 is only sufficient if $D_2 = D_0$. However, generally $D_2 \leq D_0$ is valid. Hence, an unequivocal criterion for chaotic behavior is only provided in realizing the condition $K_2 > 0$. This will be shown below.

The obtained values of $D_{2,\mathrm{max}}$ clearly show discrete changes at the critical values $(P/\Delta\lambda)_{\mathrm{crit}}$ which have been determined by the behavior of the mode correlation times. The value of $D_{2,\mathrm{max}}$ increases by an amount of approximately one, if $P/\Delta\lambda$ is driven beyond $(P/\Delta\lambda)_{\mathrm{crit}}$. This implies that the minimum number of variables which are needed to successfully model the system is increased by one if the system reaches a new structure beyond the instability at $(P/\Delta\lambda)_{\mathrm{crit}}$. Equivalently, the NDF of the system grows by the same amount.

Comparing this result with the tentative interpretation of the dynamical instabilities given in paper I, we have

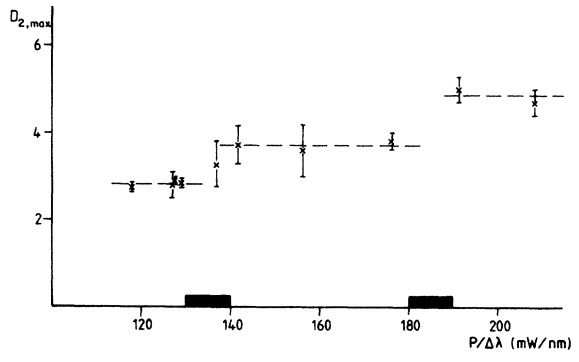

FIG. 6. Second-order dimensions $D_{2,\mathrm{max}}$ at the maximum of the laser emission in the region of low spectral power densities. On the horizontal axis, two critical spectral power densities $(P/\Delta\lambda)_{\mathrm{crit}}$ are indicated as obtained from a quick survey of the mode correlation times. At the same $(P/\Delta\lambda)_{\mathrm{crit}}$, $D_{2,\mathrm{max}}$ increases by approximately 1. The dashed lines show the mean values of $D_{2,\mathrm{max}}$ as given in Table II for each of the different ranges of $P/\Delta\lambda$ which are separated by $(P/\Delta\lambda)_{\mathrm{crit}}$.

TABLE II. Calculated mean values of $D_{2,\mathrm{max}}$ and $K_{2,\mathrm{max}}$ in three different ranges of $P/\Delta\lambda$. These mean values are shown by the dashed lines in Figs. 6 and 7. The different ranges of $P/\Delta\lambda$ are separated by those critical spectral power densities which give rise to dynamical instabilities of the mode correlation times.

	$D_{2,\mathrm{max}}$	$K_{2,\mathrm{max}}$
Range 1	2.83±0.05	1999±57
Range 2	3.71±0.11	2510±118
Range 3	4.88±0.23	2816±69

now much more evidence for the proposed model. Its essential properties have been illustrated in Fig. 2 of paper I. This model predicted a discrete change of the gain inhomogeneity at each $(P/\Delta\lambda)_{\mathrm{crit}}$. Such a change was assumed to be connected with a simultaneous alteration of the number of independently oscillating mode packets. Each of these mode packets contributes one degree of freedom to the total NDF of the system. As a consequence, it is very convincing to explain the discrete increase of $D_{2,\mathrm{max}}$ by an additional, independently oscillating mode packet whose formation is initiated at $(P/\Delta\lambda)_{\mathrm{crit}}$.

A remarkable confirmation of the fundamental relation between D_2 and the NDF of the system arises from the different values of $D_{2,\mathrm{max}}$ and $D_{2,\mathrm{abs}}$ at identical spectral power density. Until now we have only discussed the first quantity, although we have pointed out this difference already in Sec. III. Over the total range of $P/\Delta\lambda$ from 110 to 210 mW/nm, the value of $D_{2,\mathrm{abs}}$ exceeds $D_{2,\mathrm{max}}$ by an average amount of 0.84 ± 0.37. This implies that $D_{2,\mathrm{abs}}$ is larger than the next higher integer value following $D_{2,\mathrm{max}}$ for each particular spectral power density. The additional degree of freedom contributing to $D_{2,\mathrm{abs}}$ is easily identified with the influence of the absorber which is only apparent within the absorption lines in the laser emission spectrum. In order to describe the emission spectrum including the absorption lines, a particular equation is needed to account for the temporal development of the absorber number density. This parameter represents the additional degree of freedom, being responsible for the enhanced value of $D_{2,\mathrm{abs}}$ with respect to $D_{2,\mathrm{max}}$.

The change of $D_{2,\mathrm{max}}$ at both critical spectral power densities is accompanied by a discrete change of $K_{2,\mathrm{max}}$ as illustrated in Fig. 7. The different mean values for the three ranges of $P/\Delta\lambda$ are indicated in the figure. In Table II these values are shown together with their statistical errors.

Equivalent to the difference between $D_{2,\mathrm{abs}}$ and $D_{2,\mathrm{max}}$, the values of $K_{2,\mathrm{abs}}$ turned out to be significantly larger than $K_{2,\mathrm{max}}$ for each particular spectral power density. We shall give an interpretation of $K_{2,\mathrm{abs}}$ in Sec. IV C.

Since $K_2 > 0$ at each considered spectral power density, we have now complete evidence for chaotic behavior. The investigated laser system develops dissipative structures which are characterized by deterministic chaos. These structures become unstable at critical spectral power densities. The corresponding dynamical instabilities give rise

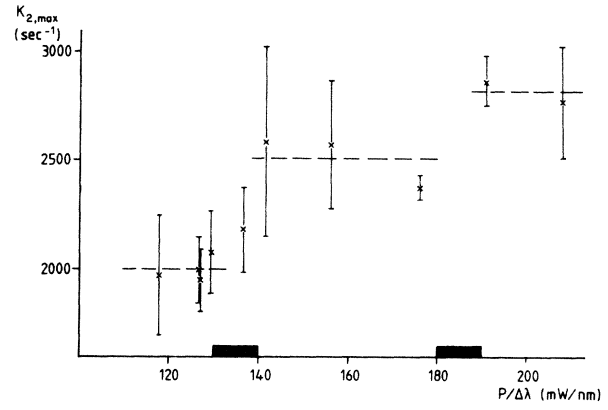

FIG. 7. Second-order entropies $K_{2,\max}$ for the same region of the spectral power density as in Fig. 6. $K_{2,\max}$ shows a significant increase at $(P/\Delta\lambda)_{\text{crit}}$ which are indicated on the horizontal axis. The dashed lines represent the mean values of $K_{2,\max}$ (see Table II) for the different ranges of $P/\Delta\lambda$.

to a new structure with a different degree of chaos (quantified by K_2) and a different NDF (quantified by D_2). The instabilities manifest themselves by a discrete change of the mode correlation time, of the correlation exponent D_2, and of the second-order entropy K_2.

Apart from the determination of D_2 and K_2 at low spectral power densities where significant instabilities occur, we also analyzed D_2 and K_2 at a high spectral power density of approximately 515 mW/nm. The examples for the determination of D_2 and K_2 given in Figs. 1—3 are derived from this situation.

As mentioned in Sec. III, at high spectral power densities we obtained $D_{2,\text{abs}} \simeq D_{2,\max}$ and $K_{2,\text{abs}} \simeq K_{2,\max}$, respectively. The value for the correlation exponent at 515 mW/nm as obtained from five successive time series was $D_2 = 2.80 \pm 0.28$. This corresponds to three degrees of freedom of the laser system at the considered high spectral power density. Since already five degrees of freedom have been obtained in the range between 185 and 210 mW/nm, we conclude that somewhere between 210 and 515 mW/nm there is a spectral power density which provides a maximal NDF. A further increase of $P/\Delta\lambda$ again simplifies the system by reducing its NDF. This behavior can be explained by such gain inhomogeneities occurring only at elevated spectral power densities. As an example, one can regard spatial hole-burning effects which are typical for standing-wave lasers with a linear cavity configuration. They usually cause a strong mode coupling with increasing spectral power density. Hence, spatial hole burning might be a reason for the low dimensionality of the laser system at high spectral power densities.

Moreover, a strong mode coupling could possibly "enslave" the additional degree of freedom which is given by the absorber. In this case, the influence of the absorber can be adiabatically eliminated, thus providing an identical NDF in an absorption dip and at the maximum of the laser emission.

B. Analogy with thermodynamical phase transitions

The purpose of this section is a detailed discussion of an important point which we already addressed in the Introduction. Usually, instabilities in systems far from thermal equilibrium appear (i) as a discrete change of an order parameter during a continuous variation of the control parameter p of the system, or (ii) as a discrete change of the derivative of an order parameter with respect to p during a continuous variation of p. The mentioned cases can be described analogous to a first- or second-order thermodynamical phase transition, respectively.

For the investigated laser system, the pump power P_{pump} serves as a control parameter, whereas the power per mode is a measure for the order parameter.[1] The power per mode is equivalent to the spectral power density $P/\Delta\lambda$.

Figure 4(b) in paper I shows the typical features of instabilities analogous to second-order phase transitions. The slope of $P/\Delta\lambda$ as a function of P_{pump} shows significant discrete changes. In paper I we have already pointed out that in those regions of P_{pump} where the slope is approximately zero, the laser emission bandwidth considerably increases together with the total output power. This behavior gives rise to a constant $P/\Delta\lambda$ within a certain range of P_{pump}.

Plotting the mode correlation times as a function of $P/\Delta\lambda$, this range of the pump power appears as a distinct value $(P/\Delta\lambda)_{\text{crit}}$. It is important to keep this in mind when considering the discontinuous changes of D_2 and K_2 as a function of $P/\Delta\lambda$. An interpretation analogous to a first-order thermodynamical phase transition would certainly be incorrect, since $P/\Delta\lambda$ cannot be regarded as a control parameter of the system.

In order to refer to thermodynamical analogies, a representation is appropriate which is given by Fig. 4 in paper I. An order parameter $(P/\Delta\lambda)$ is shown as a function of the control parameter P_{pump} of the system. At the first distinct change of the slope at $P_{\text{pump}} = 2.00$ W, the pump power seems to be no longer used to increase the power of already existing modes, but it causes a broadening of the laser-emission spectrum. At $P_{\text{pump}} = 2.25$ W, the system returns to its original behavior which is characterized by an increase of $P/\Delta\lambda$ as a function of growing P_{pump}.

The changed behavior beyond $P_{\text{pump}} = 2.00$ W can be regarded as a "redistributed" action of the input power P_{pump} within a certain range of P_{pump}. The increase of the intensity of already existing modes is postponed in favor of an enhancement of the spectral width, i.e., a formation of additional modes.

Actually, the pump power range corresponding to $(P/\Delta\lambda)_{\text{crit}}$ represents a state of the system different from the states below and beyond this range. Hence, if we consider the dynamic invariants of the system as a function of $P/\Delta\lambda$, we explicitly consider the state of the system below and beyond $(P/\Delta\lambda)_{\text{crit}}$. In these states, the system behaves according to different chaotic attractors as shown in Sec. IV A. However, dependent on the pump power the system clearly occupies a further state between these chaotic states. This "intermediate" state is entered as well as left via an instability analogous to a second-order phase

transition at two critical values of P_{pump}.

Nevertheless, the representation of the invariants as a function of $P/\Delta\lambda$ instead of P_{pump} has a reasonable motivation. A significant contribution to the limited mode correlation times is given by purely stochastic effects. It has been shown[19] that this stochastic contribution increases continuously as a function of the power per mode. Since this quantity is exactly characterized by $P/\Delta\lambda$, a representation of the mode correlation times as a function of $P/\Delta\lambda$ is appropriate to the physical situation. Indeed, the observed instabilities have been discovered by means of deviations from the purely stochastic approach. In Sec. IV C we investigate the different contributions of stochastic effects and deterministic chaos to the mode correlation time.

C. Stochastic and chaotic contributions to the mode correlation time

The origin of the limited mode correlation times in cw pumped multimode lasers has already been a subject of paper I. Briefly repeated, two different concepts have been proposed. They are based on stochastic and chaotic contributions to the behavior of the system, respectively.

The stochastic aspect has been characterized by a mean first-passage time t_{FP}. It represents the average time interval during which the considered system stays within one of several coexisting basins of attraction. The transition of the system from one basin of attraction to another one is triggered by fluctuations. A theoretical treatment of the mode correlation time within the framework of purely stochastic behavior has recently been achieved.[19] It predicts a steady decrease of the mode correlation time with increasing mode intensity. Hence, this stochastic approach cannot account for discontinuous changes of the mode correlation time at distinct $(P/\Delta\lambda)_{\text{crit}}$.

Since we have clearly demonstrated the chaotic behavior of the investigated laser system (Sec. IV A), we use the properties of deterministic chaos to develop a detailed understanding of the dynamical behavior of the laser system.

As mentioned in Sec. II B, the Kolmogorov entropy of a dynamical system is related to the inverse of the time interval τ_{corr}, during which the behavior of the system is predictable. In this sense, τ_{corr} is the correlation time of the system due to its chaotic properties. In particular, τ_{corr} limits the correlation time of a single variable of the system, as long as stochastic contributions do not prevail. Therefore, the correlation time t_{mode} of the mode intensity is expected to be influenced by the limited chaotic correlation time τ_{corr} of the system.

The three temporal quantities we deal with are the mode correlation time t_{mode}, the mean first-passage time t_{FP} (caused by purely stochastic effects), and the purely chaotic correlation time τ_{corr}. Two of these quantities are experimentally accessible: t_{mode} can be determined by means of the intracavity absorption method, and τ_{corr} can be evaluated from the Kolmogorov entropy of the system. Hence, we have a unique situation, allowing for a quantitative estimation of the influence of fluctuations on the behavior of the system. As a first step, we consider different possibilities how τ_{corr} and t_{FP} can contribute to t_{mode}.

The basis of the concerning considerations reflects the fact that the experimental observation of each one of the mentioned time scales extends over a temporal range which is very large compared with the observed temporal quantity. Therefore we always observe temporal mean values of t_{mode} as well as of τ_{corr}.

Suppose that the laser system stays in one of several coexisting chaotic attractors with a correlation time τ_{corr}. Moreover, the system shows fluctuations which exist in any dissipative system far from thermal equilibrium. These fluctuations cause the system to switch from one attractor to another after an average time interval t_{FP}. (The assumption of several coexisting basins of attraction imposes no restrictions on universality.)

(1) In the case $\tau_{\text{corr}} > t_{\text{FP}}$, the total correlation time of the system is governed by t_{FP}, since any correlation will be destroyed by a change of the attractor. The correlation time τ_{corr} within one basin of attraction is never reached in this case. For the observed mode correlation time we obtain $t_{\text{mode}} \simeq t_{\text{FP}}$ on a temporal average.

(2) The situation is somewhat different if $\tau_{\text{corr}} < t_{\text{FP}}$. The total correlation time of the system can obviously not exceed τ_{corr}. Moreover, if the correlation due to chaotic behavior vanishes after an interval τ_{corr}, the stochastic time scale further advances. If t_{FP} exceeds τ_{corr} only by a small amount, one has to consider a superposition of both time scales for an estimation of the total correlation time of the system. For $t_{\text{FP}} \gg \tau_{\text{corr}}$, the total correlation time is well approximated by the chaotic correlation time τ_{corr}.

There is a fundamental difference between the cases (1) and (2). In case (1) both stochastic and chaotic time scales are simultaneously restarted, since the change of the basin of attraction after t_{FP} destroys the correlation properties due to deterministic chaos. In case (2), however, the stochastic time scale is not influenced when τ_{corr} is reached. The simultaneous renewal of both time scales cannot happen before t_{FP} is reached.

In order to investigate the contributions of τ_{corr} and t_{FP} to the measured mode correlation times, we estimated τ_{corr} from the second-order entropy as obtained in the center of the particular absorption line which was used for the corresponding determination of t_{mode}. In this manner we obtained t_{mode} and τ_{corr} for an identical experimental situation. As a result, t_{mode} turned out to be generally less than τ_{corr}. Only the lowest spectral power densities, t_{mode} and τ_{corr} agreed within their statistical errors.

For each particular range of the spectral power density, a mean value of τ_{corr} has been calculated. The ratio of each average τ_{corr} and each particular t_{mode} then represents a measure for the influence of stochastic contributions.

In Fig. 8, this ratio is shown as a function of $P/\Delta\lambda$. At very low spectral power densities, one notices that $\tau_{\text{corr}}/t_{\text{mode}} \simeq 1$. In this situation, the mode correlation time is determined by the chaotic correlation time τ_{corr}, while $t_{\text{FP}} > \tau_{\text{corr}}$. With increasing $P/\Delta\lambda$ the mean first-passage time t_{FP} is reduced due to a growing influence of fluctuations. We obtain $\tau_{\text{corr}}/t_{\text{mode}} > 1$, since t_{FP} decreases and finally drops below τ_{corr}.

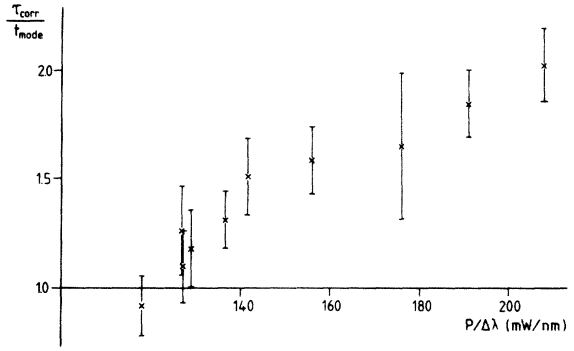

FIG. 8. Ratio of the chaotic correlation time τ_{corr}, and the mode correlation time t_{mode} as a function of the spectral power density. In order to determine τ_{corr}, the mean value of $K_{2,abs}^{-1}$ has been taken for each particular range of $P/\Delta\lambda$. The value of t_{mode} has been taken from each particular spectral power density. There are no significant steps of τ_{corr}/t_{mode} as a function of $P/\Delta\lambda$. At the lowest spectral power densities, we have $\tau_{corr}=t_{mode}$.

As an important point, we mention that the growing influence of stochastic contributions in Fig. 8 does not show the significant steps which are observed in the mode correlation times. This fact confirms the interpretation of these steps due to different chaotic correlation times in the different ranges of $P/\Delta\lambda$. Moreover, the steady increase of the stochastic contributions with increasing $P/\Delta\lambda$ is completely consistent with the stochastic approach mentioned above.

At a spectral power density of 515 mW/nm, a chaotic correlation time $\tau_{corr}\simeq 450$ μsec is obtained from K_2. This gives rise to a ratio $\tau_{corr}/t_{mode}=4.77$ for $t_{mode}=95$ μsec. In this situation, the stochastic contributions are clearly dominating. The mode correlation time at high spectral power densities is due to the mean first-passage time t_{FP}.

V. SUMMARY

Dynamical instabilities in a cw pumped, multimode-dye-laser system have been observed by means of three different key quantities of the system.

The correlation times t_{mode} of longitudinal modes has been measured by the intracavity absorption method. From the temporal evolution of the mode intensity, two invariants of the system have been extracted. They characterize its trajectory in phase space. These invariants are the second-order dimension D_2 of the attractor and the corresponding second-order entropy K_2.

The dynamical instabilities appear as discontinuities of t_{mode}, of D_2, and of K_2 at certain critical spectral power densities $(P/\Delta\lambda)_{crit}$.

From the analysis of the experimental data, sufficient conditions for deterministic chaos have been extracted. The chaotic behavior extends over the whole investigated range of the spectral power density.

The NDF of the system at different spectral power densities has been determined by the second-order dimension D_2. At low spectral power densities, the system shows only a few degrees of freedom. This fact can be explained by gain inhomogeneities, which cause a coupling of individual modes, thus giving rise to only a few independently oscillating mode packets. Below the lowest value of $(P/\Delta\lambda)_{crit}$, three degrees of freedom have been found. Both observed instabilities increase the NDF by an amount of one, respectively. This has been explained by the formation of an additional packet of independently oscillating modes at $(P/\Delta\lambda)_{crit}$. At high spectral power densities, the NDF decreases to three again. As a possible mechanism for this low dimensionality, spatial hole-burning effects have been discussed which only occur at elevated spectral power densities.

Moreover, at low spectral power densities the NDF in an absorption line exceeds the NDF as obtained at an absorption-free spectral position by an amount of one. This observation has been described by the influence of the absorber which introduces an additional degree of freedom.

By means of the second-order entropy K_2, we obtained a quantitative measure for the degree of chaos at different spectral power densities. K_2 has been used to estimate the limited correlation time τ_{corr} of the system due to its chaotic behavior. Comparing the mode correlation time t_{mode} and the chaotic contribution τ_{corr}, we determined the influence of purely stochastic contributions as a function of the spectral power density. The theoretical prediction of a steady increase of this influence with increasing spectral power density could be experimentally verified.

ACKNOWLEDGMENTS

We thank C. R. Vidal and W. Voges for efficiently programming the calculations. Support from A. Luhn in data processing is also gratefully acknowledged.

[1]H. Haken, *Synergetics—An Introduction*, 3rd ed. (Springer, Berlin, 1983).
[2]N. B. Abraham, L. A. Lugiato, and L. M. Narducci, J. Opt. Soc. Am. B 2, 7 (1985).
[3]J. R. Ackerhalt, P. W. Milonni, and M.-L. Shih, Phys. Rep. 28, 207 (1985).
[4]L. M. Lugiato and L. R. Narducci, Phys. Rev. A 32, 1576 (1985).
[5]L. W. Hillman, J. Kraszinski, R. W. Boyd, and C. R. Stroud, Jr., Phys. Rev. Lett. 52, 1605 (1984).
[6]L. M. Lugiato, L. M. Narducci, E. V. Eschenazi, D. K. Bandy, and N. B. Abraham, Phys. Rev. A 32, 1563 (1985).
[7]L. A. Westling, M. G. Raymer, M. G. Sceats, and D. F. Coker, Opt. Commun. 47, 212 (1983).
[8]H. Atmanspacher, H. Scheingraber, and C. R. Vidal, Phys. Rev. A 33, 1052 (1986).
[9]I. Procaccia, Phys. Scr. T9, 40 (1985).
[10]B. B. Mandelbrot, *Fractals—Form, Chance, and Dimension* (Freeman, San Francisco, 1977).
[11]F. Hausdorff, Math. Ann. 79, 157 (1919).
[12]P. Grassberger and I. Procaccia, Phys. Rev. Lett. 51, 346 (1983).

[13]H. Haken, Phys. Lett. **53A**, 77 (1975).
[14]P. Grassberger and I. Procaccia, Phys. Rev. A **28**, 2591 (1983).
[15]H. G. Schuster, *Deterministic Chaos* (Chemie, Weinheim, 1984).
[16]N. H. Packard, J. P. Crutchfield, J. D. Farmer, and R. S. Shaw, Phys. Rev. Lett. **45**, 712 (1980).
[17]F. Takens, in *Dynamical Systems and Turbulence, Warwick, 1980,* Vol. 898 of *Lecture Notes in Mathematics,* edited by D. A. Rand and L. S. Young (Springer, Berlin, 1981).
[18]A. Ben Mizrachi, I. Procaccia, and P. Grassberger, Phys. Rev. A **29**, 975 (1984).
[19]H. Atmanspacher, H. Scheingraber, and C. R. Vidal, Phys. Rev. A **32**, 254 (1985).